

Original paper

Melt–rock interaction as a factor controlling evolution of chromite and olivine in dunite – case study from the Kukes Massif (Mirdita ophiolite, Albania)

Jakub MIKRUT^{1*}, Magdalena MATUSIAK-MAŁEK¹, Georges CEULENEER², Michel GRÉGOIRE²,
Kujtim ONUZI³

¹ Faculty of Earth Sciences and Environmental Management, University of Wrocław, ul. Cybulskiego 30, 50-205 Wrocław, Poland; jakub.mikrut@uwr.edu.pl

² Géosciences Environnement Toulouse, Toulouse University, CNRS, IRD, 14 Avenue E. Belin, 31400 Toulouse, France

³ Institute of GeoSciences, Rr. Don Bosko, Nr.60, Tirana, Albania

* Corresponding author



The ultramafic Kukes Massif is located in the eastern part of the Mirdita ophiolite (N Albania), which is recognised as representing Supra-Subduction lithosphere. It comprises a thick (0.8–2.5 km) dunite zone containing abundant occurrences of chromite ores and is cut by orthopyroxenitic and clinopyroxenitic veins. In this paper we focus on the genesis and evolution of olivine and chromite forming dunite in the northern part of the Kukes Massif. The chemical composition of minerals in dunites is highly variable and apparent at outcrop scale. The most significant changes are recorded by olivine, which contains over 90 Fo in the host dunite but decreases to 87.5 in proximity of clinopyroxenitic veins. The composition of spinel is also sensitive to the presence of veins: in host dunite its Cr# is over 80 (chromite type I), whereas the presence of veins causes its decrease to 68 (type II). Clinopyroxene in vein-forming clinopyroxenite has Mg# from 86 to 92 and is Al-rich (Al₂O₃ 0.8–2.6 wt. %). Orthopyroxene forms orthopyroxenites (Mg# 90–93, Al₂O₃ 0.2–1.6 wt. %), but also screens (Mg# 83–91, Al₂O₃ 0.8–2.4 wt. %) at the contact between clinopyroxenite veins and the host dunite. The thick dunitic sequence at Kukes must have been formed as a result of intensive percolation of possibly boninitic melt through parental harzburgite. Another step in the evolution of the Kukes massif was related to intrusion of the pyroxenitic veins. These melts were not equilibrated with the host dunite and led to metasomatic modification of chromite and olivine, increasing Al₂O₃ content in former (from 6–8 up to 18 wt. %) and decreasing Fo (extremely from 92 to 87.5) in the latter. The process is evident proximal to clinopyroxenite veins, but a subtle effect is also recorded in the chemical composition of dunite contacting orthopyroxenite, leading to increase in Fe₂O₃ content. Metasomatism modified the composition of dunites in a zone of 0.5 m around pyroxenites. Our studies indicate a multistage evolution of the SSZ peridotites and show that its deciphering requires careful mineralogical examination.

Keywords: dunite, chromite, melt–rock interaction, Mirdita ophiolite, pyroxenitic veins

Received: 6 March 2023, *accepted:* 29 November 2023, *handling editor:* John M. Hora

1. Introduction

Thick horizons of dunites (i.e. rocks composed basically of olivine with minor amounts of other phases) are common constituents of ophiolitic massifs (e.g. Quick 1981; Nicolas and Prinzhofer 1983; Suhr et al. 2003; Pirard et al. 2013). Dunites located between the mantle peridotites and crustal gabbros and cumulates – called the Dunitic Transition Zone (DTZ) – may be derived either from processes operating in the crust, in the mantle, or both (e.g. Abily and Ceuleneer 2013; Rospabé et al. 2017; Cocomazzi et al. 2020).

Abundant chromite ore deposits are a common feature of DTZ dunites (Ceuleneer and Nicolas 1985). The origin of chromian spinel (chromite), which is the main source

of metallic chromium, is a complex issue and may be related to reaction of melts with various SiO₂ contents with host peridotite (González-Jiménez et al. 2014). Chromium content in chromite from ophiolitic complexes is highly variable (i.e. the range in Cr# – defined as atomic Cr/(Cr+Al) × 100 – is ~40–90); the highest values are known from arc-related ophiolites (Arai and Miura 2016). Primary chromite composition may be modified at later stages of the evolution of the lithosphere by metamorphism (e.g. Barra et al. 2014), hydrothermal activity (Arai and Akizawa 2014), magmatism and post-magmatic processes (Abily and Ceuleneer 2013; Bussolesi et al. 2019, 2022) or a combination of magmatic and hydrothermal activity (Rospabé et al. 2017). Since several processes can be recorded in a single chromite body, and differ-

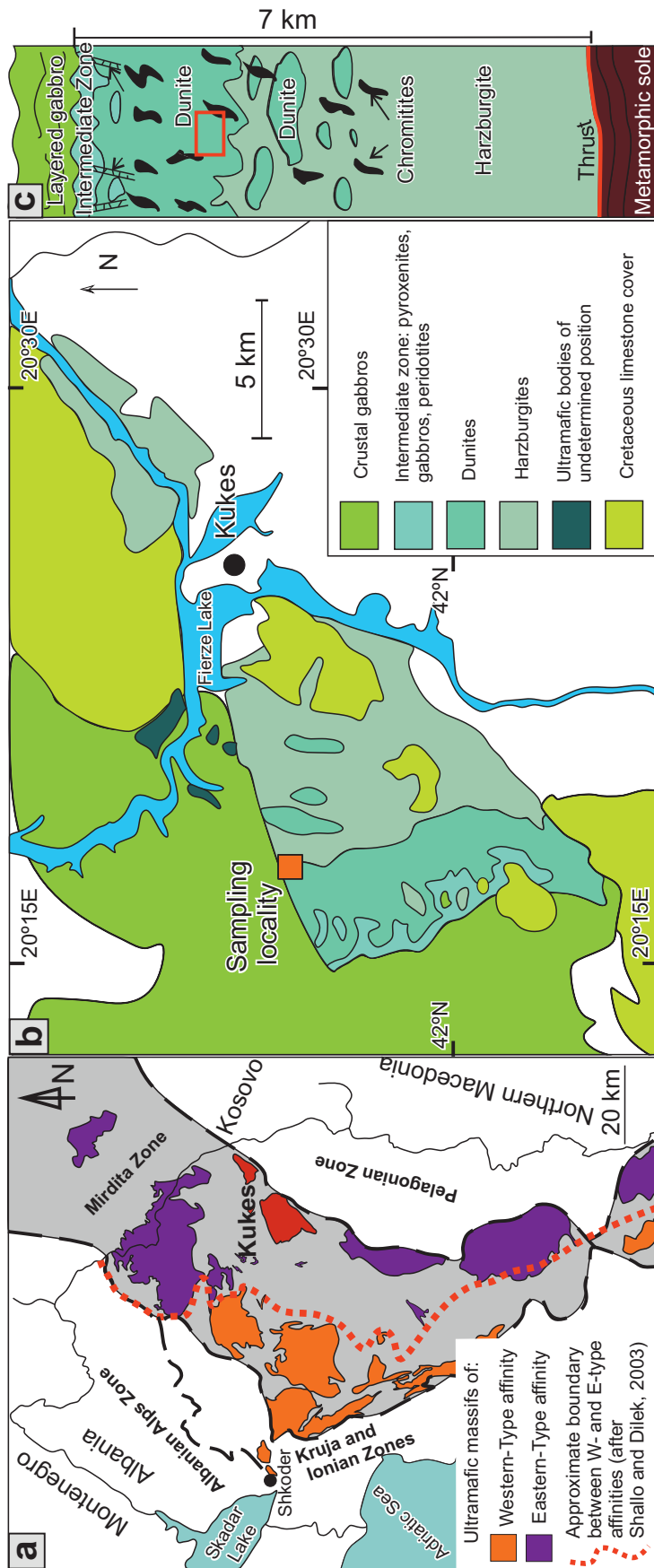


Fig. 1 a – Location of Kukes Massif (in red) within the Mirdita Zone. b – Simplified geological map of Kukes Massif with sampling locality. c – Simplified columnar section of the Kukes Massif compiled from Hoxha and Boullier (1995) and modified accordingly with our field observations and satellite images. Red frame represents approximate position of the sampling locality.

ent populations of chromites in a single host rock can record different processes, analysis of chromite composition may help to reconstruct the geological history of a massif.

Previous works discussing evolution of the peridotites from the Kukes Massif, Mirdita ophiolite, Albania commonly involved larger-scale projects focused on the genesis of the entire eastern zone of the Mirdita ophiolite (e.g. Saccani et al. 2018). Presently, only limited information on the genesis of the mantle lithologies of the Kukes massif is known from the literature (e.g. Morishita et al. 2011). Here we show that chemical composition of chromite grains dispersed within dunitic member of the Kukes Massif varies significantly even at the scale of a single outcrop. This variation has never previously been reported in the Kukes massif. This study focuses on chemical compositions of phases that form host dunitites and their cross-cutting pyroxenitic veins, in order to identify factors influencing the composition of dispersed chromite grains. This data is supported by bulk-rock analyses from three dunitites with different spatial relations relative to the pyroxenitic veins. We propose that modifications in compositions of the dispersed chromite grains and host dunitite are related to metasomatism over short length scales caused by infiltration(s) of younger silicate melts. Although chromitites are present within the Kukes massif, their composition and evolution are beyond the scope of discussion in this article.

2. Geological setting

The Mirdita ophiolite in Albania is located within the Alpine–Himalayan Orogenic Belt (Dilek and Furnes 2019; Furnes et al. 2020). Its western part, located between the Alpine–Apennine and Anatolide–Tauride mountain belts, records progression in ophiolite age from Jurassic to Cretaceous from west to east. In Albania, ophiolitic complexes are located almost entirely in the NE–SW trending Mirdita Zone, which is a remnant of the Neothetian Pindos–Mirdita basin (Dilek et al. 2005; Fig. 1a).

The Mirdita ophiolite consists of multiple ultramafic massifs, arranged in two parallel N–S trending belts (op. cit., Nicolas et al. 1999; Xiong et al. 2015; Bussolesi et al. 2022). They are separated by a ~30 km wide zone of volcanic and plutonic rocks also belonging to the ophiolitic sequence. Several horizontal Jurassic and Cretaceous marine sedimentary complexes transgressively cover the volcanic rocks, suggesting that the ophiolite escaped major tectonic deformations and that its present position corresponds to the oceanic topography (Nicolas et al. 2017). Another remarkable feature of Mirdita ophiolite is a change of geochemical affinity from Mid-Ocean Ridge (MOR, in the western part of Mirdita ophiolite) to Supra-Subduction Zone (SSZ, in eastern part of the ophiolite), which was identified within volcanic and plutonic complexes (e.g. Shallo and Dilek 2003; Dilek et al. 2008 and references therein).

The ultramafic Kukes Massif is located in the northern part of the Mirdita ophiolite and belongs to its eastern (i.e. of SSZ affinity) domain (Fig. 1a). The mantle sequence begins (from the bottom) with harzburgite which grades to dunite. The lowermost dunites form lenses within harzburgite and olivine abundance increases upwards. The result is an exceptionally thick (estimations range from 800 m to 2.5 km; Hoxha and Boullier 1995) zone of massive dunite (Fig. 1b, c). High temperature deformation structures of ultramafic rocks are dominant, but low temperature deformation could be locally superimposed (Op. cit.). Chromitite lenses and pods are common within the whole dunite zone but occur also in the uppermost harzburgite, which makes the Kukes Massif of great economic interest (Steblez 1994). The thickness of the preserved mantle column is estimated to exceed 6–7 km (Hoxha and Boullier 1995). Gabbros lie on dunite or are separated by the “intermediate

zone”, formed of pyroxenites and cumulative peridotites (Fig. 1c).

Several previous studies on mineral chemistry of eastern Mirdita dunites were conducted. They point to the development of ultramafic massifs in a (proto) forearc setting (Saccani and Tassinari 2015; Xiong et al. 2015) and formation of dunites and chromitite related to percolation of boninite (Morishita et al. 2011) or hybrid melt formed due to reaction of SiO_2 -rich melt and peridotite (Junge et al. 2021). Saccani et al. (2018) proposed a model for development of peridotites within Mirdita ophiolite, linked to multiple melting events and episodes of subduction-related metasomatic enrichment.

3. Methodology

This study is based on 9 dunite samples obtained from the lowermost part of the dunitic member of the Kukes Massif, from a locality near an active chromite mine (Fig. 1a, approximate location $42^\circ 03' 54.8'' \text{N } 20^\circ 17' 20.2'' \text{E}$). Seven samples of dunites (named KP) were collected along a 5.5 m long profile (Fig. 2). The dunites are locally cross-cut by up to 10 cm thick pyroxenitic veins: sample

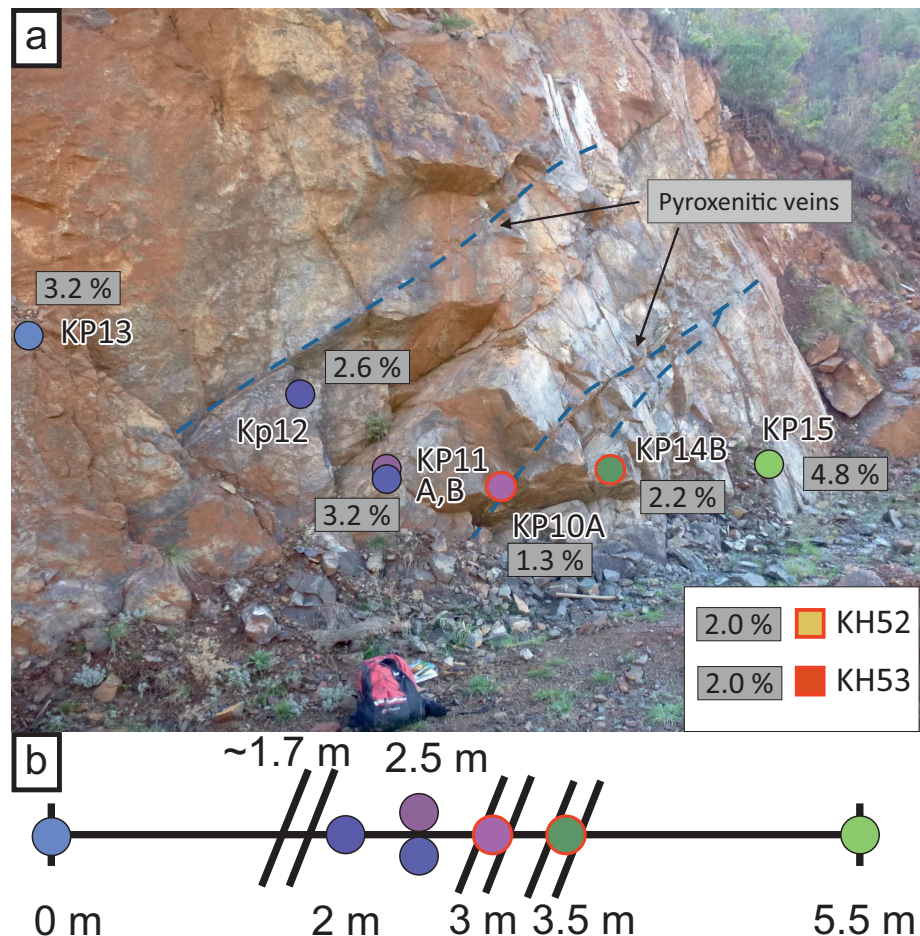


Fig. 2 Field relationships between veins and the host dunite. **a** - Occurrence of the veins in the studied outcrop with sample locations. Symbols with bold red edge represent dunites with pyroxenitic veins. Numbers in grey fields indicate modal content of spinel. **b** - Schematic profile showing spatial relationships between samples. Parallel lines marks pyroxenitic veins.

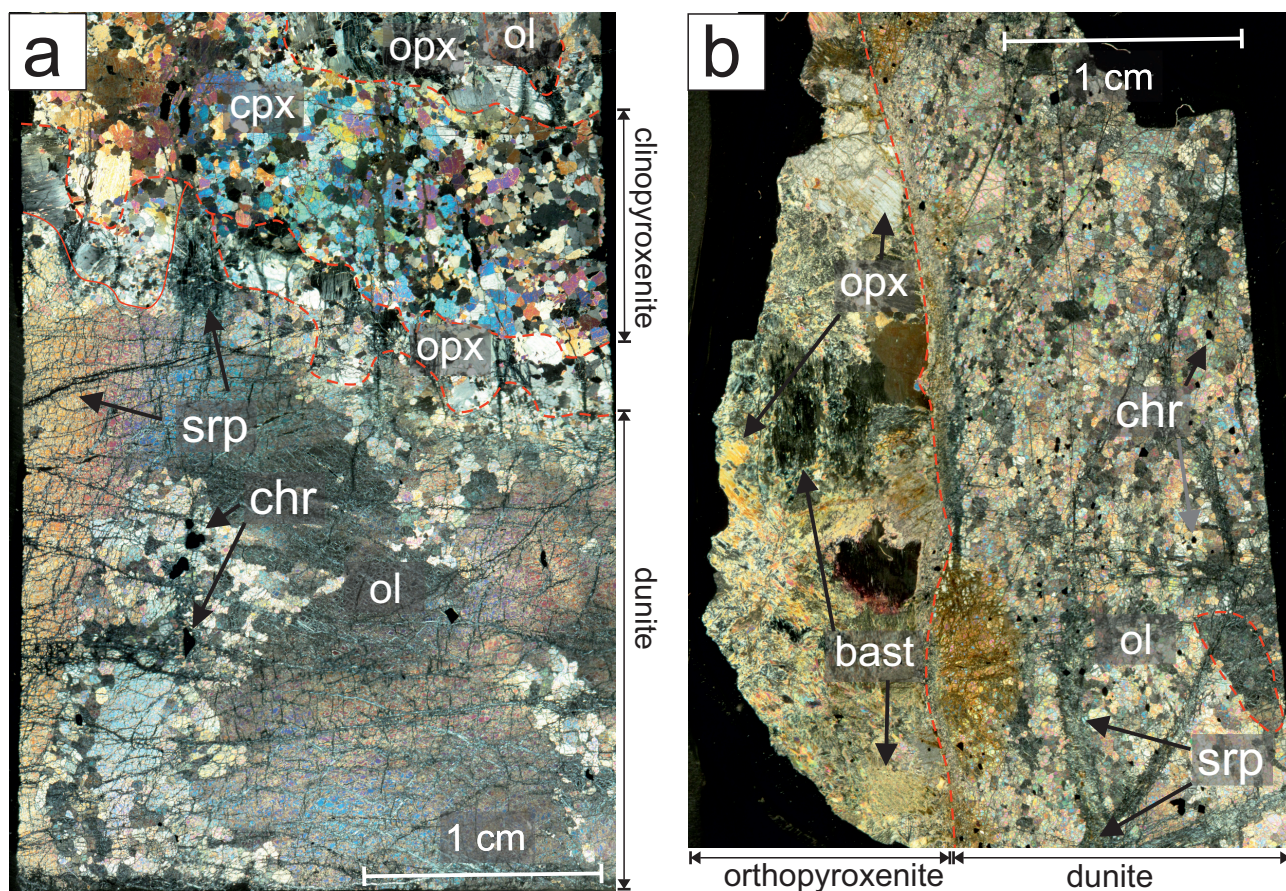


Fig. 3 Petrographic features of host dunite and pyroxenitic veins. **a** - Microphotograph of a thin section of dunite KH53 with clinopyroxenite vein (crossed-polars). Note the presence of orthopyroxene screen at the contact with the host dunite. **b** - Microphotomicrograph of dunite KP10A with orthopyroxenite vein; dunite comprise porphyroclasts of olivine (one marked with dashed lines), serpentine locally form channel-like structures (crossed-polars). Mineral abbreviations: ol – olivine, chr – chromite, opx – orthopyroxene, cpx – clinopyroxene, srp – serpentines, bast – bastite.

KP10A is cut by orthopyroxenite, and sample KP14B is cut by clinopyroxenite. Sample KP12 is proximal to a pyroxenitic vein (Fig. 2b), while samples KP11 (A, B), KP13 and KP15 are distal from the veins. The sample-set forming profile is complemented with 2 dunites (KH52 and KH53) from the distant (i.e. >15 m apart) part of the outcrop; those samples are also cut by thin (<2 cm) veins: sample KH52 is cut by orthopyroxenite, while KH53 is cut by clinopyroxenite (Fig. 3a).

Thin sections of rocks were investigated under a polarised light microscope in transmitted and reflected light. Modal content of chromite was obtained on a high quality image by point-counting method on a basis of 300 points using JMicroVision software (Roduit 2007). In situ major element compositions of minerals were measured by electron microprobe using the Cameca SX 100 and the Cameca SXFive (Faculty of Geology, University of Warsaw, Poland) as well as the Jeol JXA8530F Hyperprobe Field Emission Electron Probe Microanalyser (Department of Earth Sciences, Uppsala University, Sweden). All the used microprobes worked under standard conditions with a 15 kV accelerating voltage, beam current 15 nA

and counting times 10 or 20 s, increased to 40 s for Ni and Ca in olivine to improve detection limits. Automatic profiles were acquired for veins in samples KH52 and KH53 using the Cameca SXFive at the “Centre de Micro-Caractérisation Raimond Castaing” in Toulouse, France. Two profiles were obtained for each sample, with an analytical step of 55 μm . The following standards were applied: wollastonite for Si and Ca, rutile (Warsaw) or pyrophanite (Toulouse, Uppsala) for Ti, orthoclase (Warsaw) or Al_2O_3 (Toulouse, Uppsala) for Al, fayalite (for olivine in Uppsala) or Fe_2O_3 for Fe, rhodonite (Warsaw) or pyrophanite (Toulouse and Uppsala) for Mn, albite for Na, metallic or oxide Ni, Cr_2O_3 for Cr, and MgO for. Detection limits are: 480 ppm for Si, 70 ppm for Ti (290 for automatic profiles in Toulouse), 140 ppm for Al (440 ppm in Toulouse), 300 ppm for Fe (1040 ppm in Toulouse), 90 ppm for Cr (330 in Toulouse), 250 ppm for Ni (1060 ppm in Toulouse), 220 ppm for Mn (980 ppm in Toulouse), 250 ppm for Mg (410 ppm in Toulouse), 90 ppm for Ca (740 ppm in Toulouse).

Bulk rock composition was analysed for three dunites. Their composition was analysed at Bureau Veritas

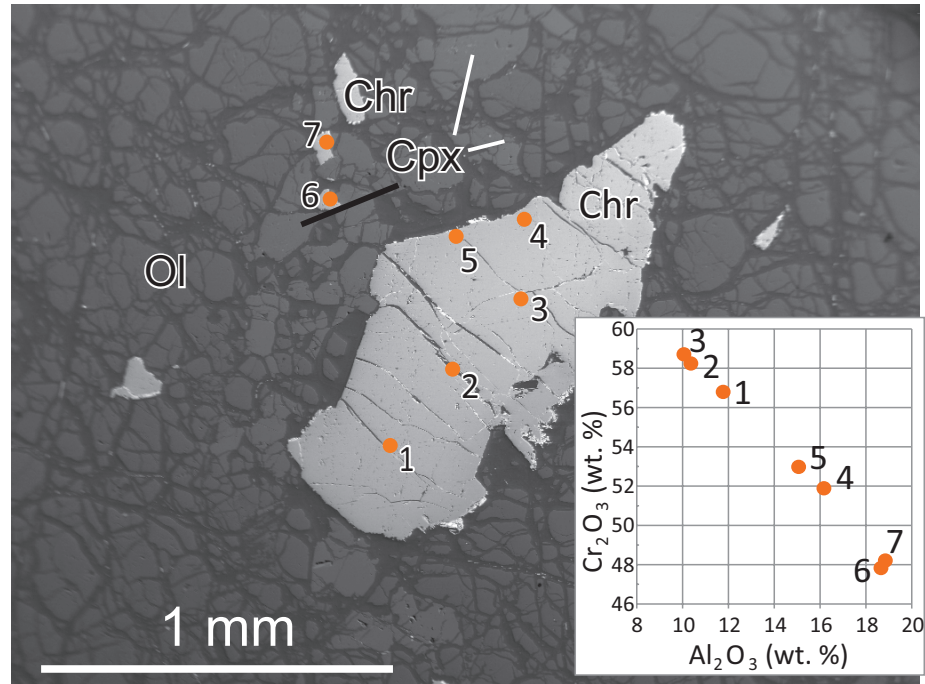


Fig. 4 Backscattered electron image of a large chromite grain from sample KP14B. Note the presence of small interstitial clinopyroxene. Inset diagram shows variability of Cr_2O_3 and Al_2O_3 content within chromite grains, analytical spots locations correspond to the points on the diagram.

laboratories (Vancouver, Canada) by Inductively Coupled Plasma Mass Spectrometry (procedure code LF202).

Forsterite (Fo) content of olivine is calculated as atomic $\text{Mg}/(\text{Mg} + \text{Fe}) \times 100$ per olivine formula unit. The Mg-number (Mg#) of chromite and pyroxenes denotes the atomic ratio of $\text{Mg}/(\text{Mg} + \text{Fe}^{2+}) \times 100$, while Cr# of chromite denotes the atomic ratio of $\text{Cr}/(\text{Cr} + \text{Al}) \times 100$. Contents of Fe^{3+} and Fe^{2+} in spinel were calculated by charge balance (Deer et al. 1993).

4. Results

4.1. Field and petrographic observations

The studied outcrop within the Kukes Massif is composed of dunite with no macroscopically visible foliation. It hosts locally folded, 1 to 10 cm thick layers and schlieren of chromitite with diffuse contacts with the peridotite. The peridotite is also cross-cut by numerous, 1.5 to 10 cm thick, pyroxenitic veins with a sharp contact (Fig. 2a). All collected samples are orthopyroxene-free dunite with subordinate chromite, scarce (<1% in modal composition) interstitial clinopyroxene and negligible amounts of sulfides (Fig. 3a, b). Orthopyroxene is present only as a screen on contact with clinopyroxenitic veins. Pervasive serpentinitisation is widespread but variably developed – locally it forms channel-like structures ignoring rock-foliation and olivine boundaries (Fig. 3b). Olivine forming dunites are either scarce megacrystic porphyroblasts (200 μm to 2 cm long) or 30 to 200 μm long neoblasts; the contact between the two types of olivine is undulatory

(Fig. 3a, b). Elongated grains of both types of olivine are locally parallel and define weak foliation. The poikilitic megacrysts enclose crystals of chromite arranged in parallel streaks, neoblasts locally enclose single grains of chromite.

Chromite is a subordinate phase and constitutes between 0.3 and 5% of the rock, with slightly lower abundances near veins and the highest in distal dunites (Fig. 2a). Grains of chromite are usually isometric and between 30 and 500 μm in diameter, while scarce larger (up to 2 mm) grains are elongated. They occur both as interstitial and enclosed grains within recrystallised olivine. Some of the chromite grains contain <20 μm inclusions of amphibole, olivine, ortho- and clinopyroxenes. Scarce magnetite occurs along margins and cracks within chromite and within serpentinite veins.

Clinopyroxene in dunite forms anhedral, interstitial grains with size from 50 to 400 μm (Fig. 4). Only in one dunite (KP11B) some clinopyroxene grains reach up to 800 μm . Clinopyroxene is always associated with chromite, either in direct contact or in close proximity.

Foliation in few dunites (KP10A, KP14B, KH52 and KH53) is cross-cut at high angles by pyroxenitic, variably altered veins. Clinopyroxenitic veins in samples KP14B and KH53 have complex structure (Fig. 3a): their cores are composed of clinopyroxenitic accumulates, while the margins are underlined by up to 5 mm thick screens of orthopyroxene with some resorbed olivine grains. Some clinopyroxene in the inner part of the veins is enveloped by tremolite. The orthopyroxenite veins (KP10A, KH52) are heavily altered, orthopyroxene is often transformed to bastite (Fig. 3b), those veins com-

Tab. 1 Representative chromite analyses in dunites (presented in wt. %) and their recalculations to structural formulae (C=3). FeO* refers to total iron oxides measured by microprobe. Contents of Fe³⁺ and Fe²⁺ were calculated by charge balance (Deer et al. 1993).

Sample	KP10A	KP10A	KP14B	KP14B	KP15	KP12	KP11A	KH53	KH53	KH52	KH52
Spinel type	II	II	II	II	I	I	I	II	II	II	II
SiO ₂	b.d.l.	0.79	0.12	b.d.l.	b.d.l.						
TiO ₂	0.07	0.11	0.15	0.12	0.08	0.11	0.10	0.13	0.07	0.03	0.06
Al ₂ O ₃	12.64	10.94	16.17	10.06	6.57	7.94	6.85	18.37	9.72	14.16	13.77
Cr ₂ O ₃	55.35	57.30	51.89	58.71	59.36	60.51	61.77	49.77	58.54	52.30	53.87
FeO*	23.74	23.35	22.61	22.48	25.76	24.08	23.33	20.36	19.39	22.43	20.46
MnO	0.36	0.34	0.59	0.39	0.39	0.55	0.40	0.38	0.44	0.28	0.24
NiO	0.04	b.d.l.	0.09	b.d.l.	0.03	b.d.l.	b.d.l.	0.09	0.03	0.05	b.d.l.
MgO	7.39	7.85	8.91	7.93	6.91	7.13	7.48	9.32	8.84	8.65	9.03
CaO	b.d.l.										
Total	99.59	99.989	100.41	99.769	99.10	100.31	99.93	99.21	97.15	97.90	97.43
Si ⁺⁴	-	-	-	-	-	-	-	0.025	0.004	-	-
Ti ⁺⁴	0.002	0.003	0.004	0.003	0.002	0.003	0.003	0.003	0.002	0.001	0.002
Al ⁺³	0.495	0.432	0.612	0.396	0.267	0.316	0.275	0.692	0.391	0.556	0.543
Cr ⁺³	1.454	1.500	1.318	1.549	1.616	1.614	1.660	1.258	1.578	1.378	1.425
Fe ⁺³	0.050	0.072	0.060	0.061	0.113	0.069	0.062	-	0.021	0.064	0.029
Fe ⁺²	0.610	0.567	0.547	0.566	0.628	0.611	0.602	0.556	0.532	0.561	0.544
Mn ⁺²	0.010	0.011	0.016	0.011	0.011	0.016	0.011	0.010	0.013	0.008	0.007
Ni ⁺²	0.001	-	0.002	-	0.001	-	-	0.002	0.001	0.001	-
Mg ⁺²	0.366	0.401	0.427	0.395	0.355	0.359	0.379	0.444	0.449	0.430	0.450
Ca ⁺²	-	-	-	-	-	-	-	-	-	-	-
total	2.989	2.986	2.987	2.982	2.994	2.987	2.992	2.991	2.990	3.000	3.000
Cr#	74.6	77.7	68.3	79.7	85.8	83.6	85.8	64.5	80.2	71.2	72.4
Mg#	35.7	38.5	41.3	38.6	32.3	34.6	36.4	44.9	44.8	40.7	44.0
Fe ₂ O ₃	2.18	2.78	2.64	2.55	4.45	2.76	2.42	0.00	0.56	2.55	1.12
FeO	21.78	20.85	20.23	20.18	21.76	21.59	21.16	20.36	18.88	20.14	19.45

prise minor amounts of small (<250 µm) clinopyroxene grains. At the contact with veins, small grains of olivine are present (Fig. 3a, b).

4.2. Chemical composition of chromite

In total 50 chromite and Al-chromite grains were analysed with electron microprobe and their representative analyses are given in Tab. 1. Variations in chemical composition of chromite occur at various scales (outcrop, hand specimen or even within a single grain). Two compositional types of chromite were identified (Tab. 1, Fig. 5). The first type is formed of chromite *sensu stricto* (Fig. 5a) and is characteristic of chromite occurring in dunite and located at least 0.3 m from pyroxenitic veins. This group is characterised by a high Cr₂O₃ content (56–62 wt. %), constant Al₂O₃ content (6–8 wt. %, Fig. 5b) resulting in high Cr# (82–87), and Mg# between 25–40 (Fig. 5c). The second type of chromite (with composition ranging between pure and Al-chromite, Fig. 5a) occurs in dunites cross-cut by pyroxenitic veins (Fig. 2). Chromite grains of this type have generally lower Cr₂O₃ content (48–60 wt. %) negatively correlated with that of Al₂O₃ (9–19 wt. %); Al₂O₃ contents exceeding 14 wt. % occur only in grains close to veins. The Cr# in this type is

strongly variable (between 62 and 81) and Mg# is higher than in the first group (25–49).

Differences in chromite composition are observed in thin-section scale between dunites cross-cut by clino- and orthopyroxenite veins (Fig. 5d). The largest chromite grain in the dunite cross-cut by clinopyroxenite (KP14B) has Cr₂O₃-rich, TiO₂- and Al₂O₃-poor core (57–59, 0.12–0.13 and 10–12 wt. %, respectively), while the rim is depleted in Cr₂O₃ and enriched in TiO₂ and Al₂O₃ (52–53, 0.15 and 15–16 wt. % respectively, Fig. 4). Small chromite grains are richer in Al₂O₃ (19 wt. %) than rims of larger ones. Within 2 cm from vein, Cr# of chromite increases along with decreasing Ti towards the dunite (from 64 to 78 and from 0.19 to 0.14 wt. %, respectively). In the dunite cross-cut by orthopyroxenite (KP10A) the Cr# in chromite increases with distance from the vein (from 75 to 78) but, conversely to KP14B, it is positively correlated with the TiO₂ content (from 0.07 to 0.14 wt. % towards dunite, Fig. 5d).

4.3. Chemical composition of olivine

In total 83 olivine grains were analysed by electron microprobe. Representative analysis are shown in Tab. 2. The Fo content in dunitic olivine varies between 87.5

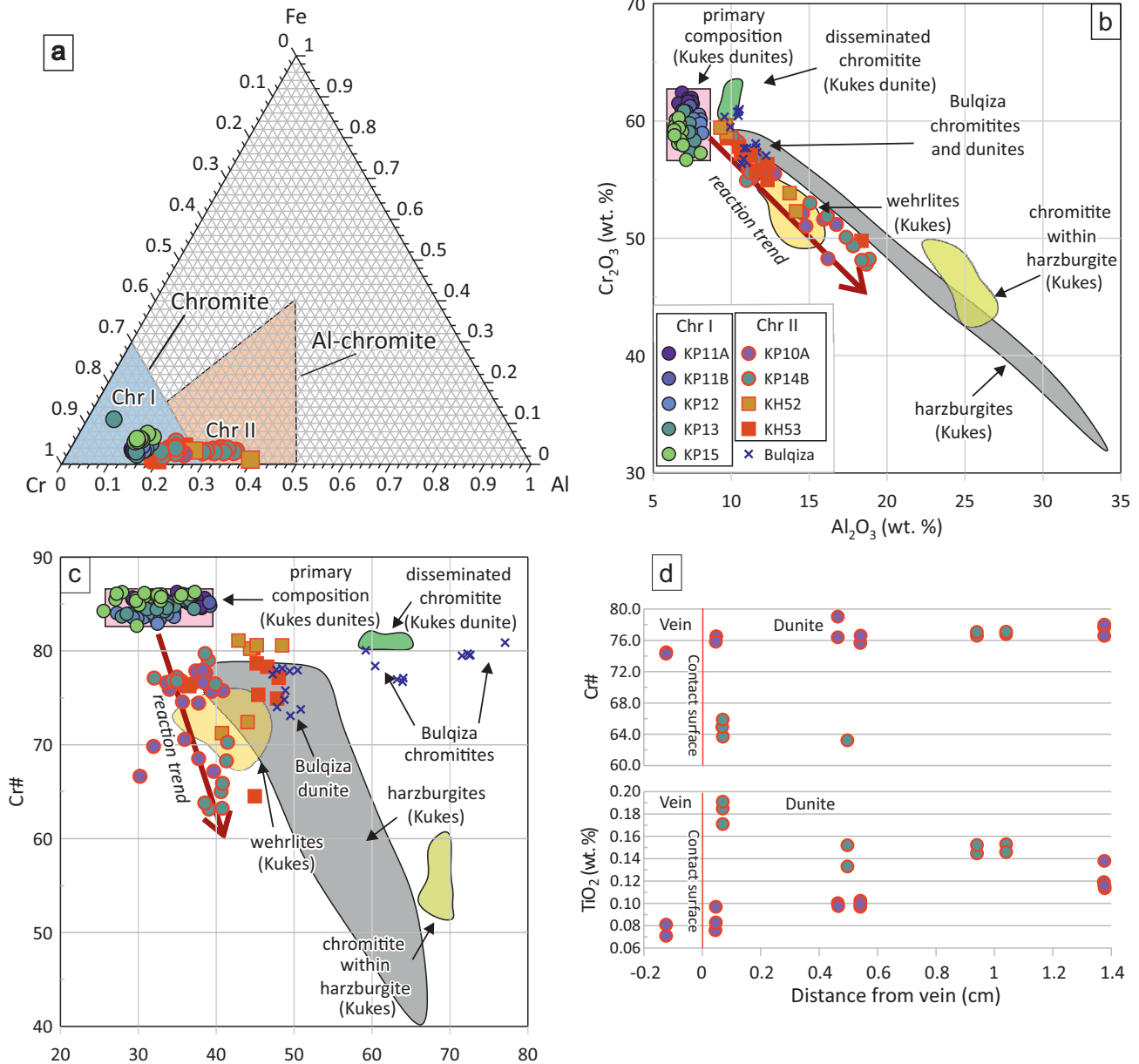


Fig. 5 Chemical composition of spinel. **a** –Ternary classification diagram of spinels. **b** - Relation between Al_2O_3 and Cr_2O_3 contents. **c** - Cr# - Mg# relationships. **d** – Profiles illustrating Cr# and TiO_2 contents in samples KP10A and KP14B changing with the distance from pyroxenitic veins; “harzburgites”, “wehrlites” and “chromitites” fields mark composition range of spinel from those rocks within the whole Kukes massif (J. Mikrut unpublished data), data for Bulqiza is from Xiong et al. 2015.

and 92.5 and NiO content varies from 0.15 to 0.42 wt. % (Tab. 2, Fig. 6); in dunites with pyroxenitic veins the Fo content in most cases increases from the vein towards the dunite (from 87.5 to 92, an example of this behaviour is shown on profile on Fig. 7d). The lowest values of Fo (87.5–88.5) are observed in olivine in dunites cross-cut by clinopyroxenite veins (KH53 and KP14B) at the margin of the vein, whereas the highest values (91.5–92.5) are present in dunite (KH52) cut by orthopyroxenite. Dunites from the profile, but not in direct contact with veins, have intermediate Fo values (89.5–91.5).

4.4. Chemical composition of pyroxenes

In total 38 orthopyroxene and 80 clinopyroxene grains were analysed by electron microprobe and their representative analyses are given in Tab. 3. Clinopyroxene (mostly diopside with some augite grains) occurs as an interstitial phase within some of the dunites and in pyroxenitic veins (Tab. 3, Fig. 7c). Composition of interstitial clinopyroxene from the dunites exhibits negative correlation between Mg# (92.0–97.0) and both, Al_2O_3 (<1 wt. %) and Cr_2O_3 contents (0.05–0.4 wt. %; Fig. 7a, b), fur-

Tab. 2 Representative olivine analyses (presented in wt. %) and their recalculations to structural formulae ($O^{2-}=4$).

Sample	KP14B	KP14B	KP10A	KP10A	KP12	KP11B	KH53	KH53	KH52	KH52
SiO ₂	40.56	40.98	40.93	41.03	41.17	41.35	41.09	40.64	41.02	41.23
TiO ₂	b.d.l.	0.02	b.d.l.							
Al ₂ O ₃	b.d.l.									
Cr ₂ O ₃	b.d.l.	b.d.l.	0.03	b.d.l.						
FeO*	11.49	10.51	10.62	9.13	9.86	8.38	8.74	9.21	7.71	7.86
MnO	0.18	0.17	0.23	0.15	0.22	0.11	0.13	0.14	b.d.l.	b.d.l.
NiO	0.24	0.16	0.24	0.28	0.23	0.22	0.29	0.32	0.26	0.26
MgO	47.92	48.88	48.86	50.06	48.80	50.23	48.71	48.54	50.71	50.98
CaO	0.01	0.01	0.03	0.02	0.03	0.03	0.03	0.02	b.d.l.	0.03
Total	100.41	100.73	100.95	100.70	100.34	100.32	99.00	98.87	99.73	100.40
Si ⁺⁴	0.998	1.000	0.998	0.996	1.005	1.003	1.011	1.005	0.998	0.997
Ti ⁺⁴	-	-	-	-	-	-	-	-	-	-
Al ⁺³	-	-	-	-	-	-	-	-	-	-
Cr ⁺³	-	-	0.001	-	-	-	-	-	-	-
Fe ⁺²	0.236	0.214	0.217	0.185	0.201	0.170	0.180	0.190	0.157	0.159
Mn ⁺²	0.004	0.004	0.005	0.003	0.005	0.002	0.003	0.003	-	-
Ni ⁺²	0.005	0.003	0.005	0.006	0.004	0.004	0.006	0.006	0.005	0.005
Mg ⁺²	1.758	1.778	1.775	1.812	1.777	1.816	1.788	1.789	1.839	1.838
Ca ⁺²	-	-	0.001	-	0.001	0.001	0.001	-	-	0.001
total	3.001	2.999	3.002	3.003	2.994	2.997	2.988	2.995	3.000	3.000
Fo	88.16	89.26	89.11	90.74	89.84	91.44	90.86	90.38	92.14	92.04

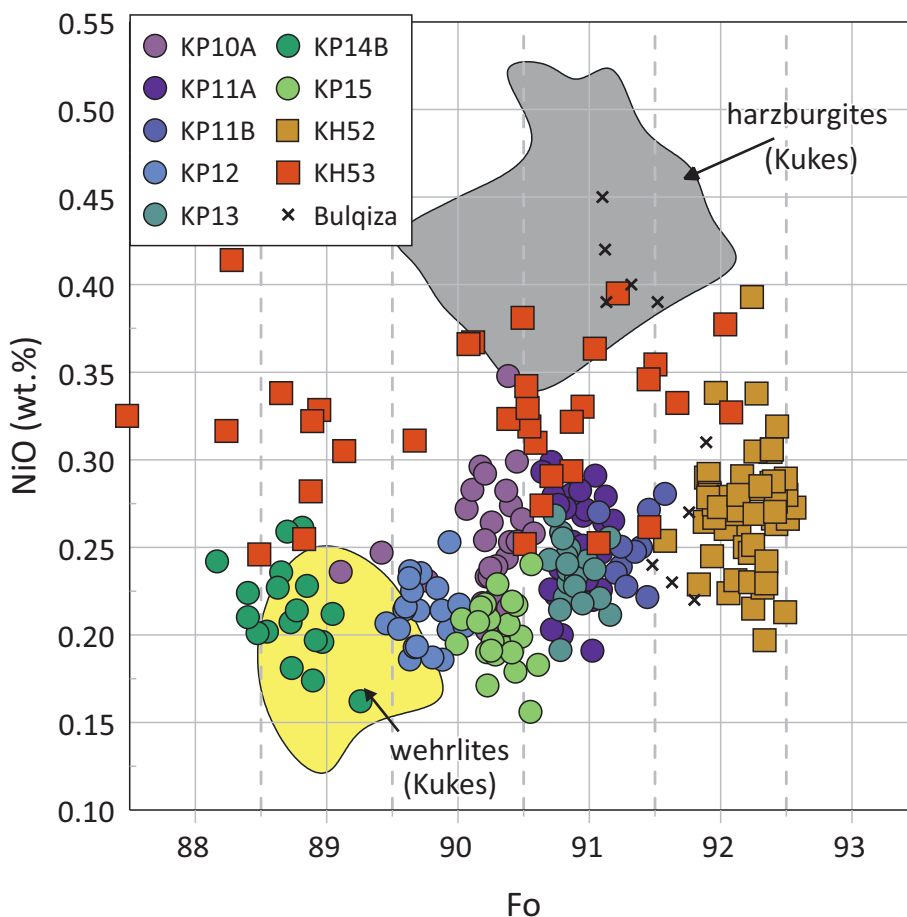
thermore it has lower content of ferrosillite endmember than clinopyroxene in veins (Fig. 7c). Diopside forming

clinopyroxenites has Mg#=84.4-94.0 which increases towards margins of the veins (e.g., KH53, Figs 3a, 7d).

The Al₂O₃ content in clinopyroxene from clinopyroxenite varies from 0.90 to 2.70 wt. %, whereas Cr₂O₃ content is <0.25 wt. %, and is not correlated with location within the vein. Single grains of clinopyroxene (diopside) found within orthopyroxenite (KP10A, KH52) have high Mg#=93.5–96.5 and Cr₂O₃ (0.40–0.55 wt. %) content, but low Al₂O₃ concentrations (<0.7 wt. %).

Composition of orthopyroxene (enstatite, Fig. 7c) varies between those forming screens in clinopyroxenites and those forming orthopyroxenites (Tab. 3, Fig. 8a, b). The former has low but strongly variable Mg# (82.5–91.0), high Al₂O₃

Fig. 6 Forsterite – NiO relations in olivine. “harzburgites” and “wehrlites” fields mark composition range of olivine from those rocks within Kukes massif (J. Mikrut unpublished data). Circles mark samples collected from the profile, squares – additional two samples with complete veins cross-sections.



Tab. 3 Representative pyroxene analyses (presented in wt. %) and their recalculations to structural formulae ($O^{2-}=6$)

Sample	KP10A	KP11A	KP14B	KH53	KH53	KP10A	KP14B	KH52	KH53	KH53
Lithology	Vein-Opxt	Dunite	Vein-Cpxt	Dunite	Vein-Cpxt	Vein-Opxt	Vein-screen	Vein-Opxt	Vein-screen	Vein-screen
SiO ₂	53.97	55.42	53.28	52.95	53.13	57.25	55.48	57.77	56.72	55.97
TiO ₂	0.02	0.02	0.08	0.08	0.05	0.02	0.03	0.05	0.03	0.03
Al ₂ O ₃	0.67	0.11	1.82	1.85	1.83	0.74	1.97	0.56	1.87	1.70
Cr ₂ O ₃	0.45	0.12	0.16	0.18	0.17	0.37	0.14	0.24	0.16	0.12
FeO*	1.88	1.24	4.84	2.58	4.58	6.53	9.03	5.06	6.01	7.87
MnO	0.08	0.05	0.13	0.12	0.16	0.15	0.28	0.08	0.14	0.22
NiO	0.03	b.d.l.	0.06	0.06	0.07	b.d.l.	0.08	0.05	0.06	0.08
MgO	17.95	17.91	17.35	16.59	17.62	34.75	32.35	34.83	33.86	31.93
CaO	24.88	25.81	22.56	24.38	22.00	0.45	0.45	0.35	0.36	0.56
Na ₂ O	0.08	b.d.l.	0.10	b.d.l.	0.08	b.d.l.	b.d.l.	b.d.l.	b.d.l.	b.d.l.
Total	100.03	100.68	100.42	98.80	99.69	100.30	99.89	99.01	99.20	98.48
Si ⁺⁴	1.964	1.995	1.944	1.952	1.947	1.972	1.943	2.004	1.967	1.974
Ti ⁺⁴	0.001	0.001	0.002	0.002	0.001	–	0.001	0.001	0.001	0.001
Al ⁺³	0.029	0.005	0.078	0.081	0.079	0.030	0.081	0.023	0.076	0.071
Cr ⁺³	0.013	0.003	0.005	0.005	0.005	0.010	0.004	0.007	0.004	0.003
Fe ⁺²	0.057	0.037	0.148	0.080	0.140	0.188	0.265	0.147	0.174	0.232
Mn ⁺²	0.003	0.002	0.004	0.004	0.005	0.004	0.008	0.002	0.004	0.007
Ni ⁺²	0.001	–	0.002	0.002	0.002	–	0.002	0.001	0.002	0.002
Mg ⁺²	0.974	0.961	0.943	0.912	0.963	1.784	1.689	1.801	1.750	1.678
Ca ⁺²	0.970	0.995	0.882	0.963	0.864	0.017	0.017	0.013	0.013	0.021
Na ⁺¹	0.006	–	0.007	–	0.005	–	–	–	–	–
total	4.017	3.9980	4.017	4.001	4.012	4.006	4.012	4.000	3.992	3.989
Mg#	94.5	96.3	86.4	92.0	87.3	90.5	86.4	92.5	90.9	87.8
Wo	48.48	49.92	44.70	49.26	43.92	0.85	0.86	0.66	0.67	1.09
En	48.68	48.22	47.80	46.65	48.96	89.69	85.69	91.84	90.35	86.90
Fs	2.85	1.86	7.50	4.09	7.12	9.45	13.44	7.50	8.98	12.01

(0.90–2.70 wt. %) and low Cr₂O₃ contents (typically <0.20 wt. %, with a single analysis <0.32 wt. %); Mg# and Cr₂O₃ are positively correlated along a hyperbolic trend (Fig. 8b). Orthopyroxene forming screens enveloping clinopyroxenitic veins has the lowest Mg# close to the axis of the vein and the highest at contact with the host dunite (Fig. 7d). Orthopyroxene in orthopyroxenitic veins has elevated Mg# (90.1–93.0) and Cr₂O₃ content (0.05–0.45 wt. %), but is Al-poor (Al₂O₃ = 0.20–1.20 wt. %; rarely ≤2.60 wt. %). Mg# is positively correlated with Al₂O₃ and Cr₂O₃ contents, but no correlations were observed between the composition and textural position of grains within veins. As higher Mg# values are observed within orthopyroxenites, their composition is more enstatitic than those forming screens (Fig. 7c).

4.5. Bulk-rock composition

Bulk-rock composition was determined for three dunites with different spatial relations to pyroxenite. These were located at the contact with orthopyroxenitic vein (KP10), around 0.5 m from pyroxenitic vein (KP11) and over 1.5 m from any observable vein (KP13, Fig. 2b). Analyses are given in Tab. 4. Samples are moderately serpentinised (Lost On Ignition (LOI) = 7.4–8.2 wt. %).

The MgO content slightly increases with distance from vein (from 43.85 wt. % to 44.16 wt. %), conversely to Fe₂O₃ content (9.37 wt. % nearby contact and 8.92–8.93 wt. % at distance from vein, Fig. 9a; data presented in diagrams is LOI normalised). The Al₂O₃ content is low (0.10–0.17 wt. %, Fig. 9b), which is consistent with the absence of orthopyroxene. Dunites are CaO⁻ (0.14–0.19 wt. %) and alkali-poor (below detection limits). Most of trace elements concentrations are below detection limits.

5. Discussion

An influence of MORB and boninitic melts on the evolution of the Kukes Massif was identified by Morishita et al. (2011), who linked change in the nature of the melt with prograding subduction. However, the composition of the protolith peridotites remains unclear. Also, the influence of the infiltrating melts on the dunites remains ambiguous.

5.1. Origin of dunite

One of the most striking features of the Kukes Massif is the thickness of the dunitic mantle–crust transition zone,

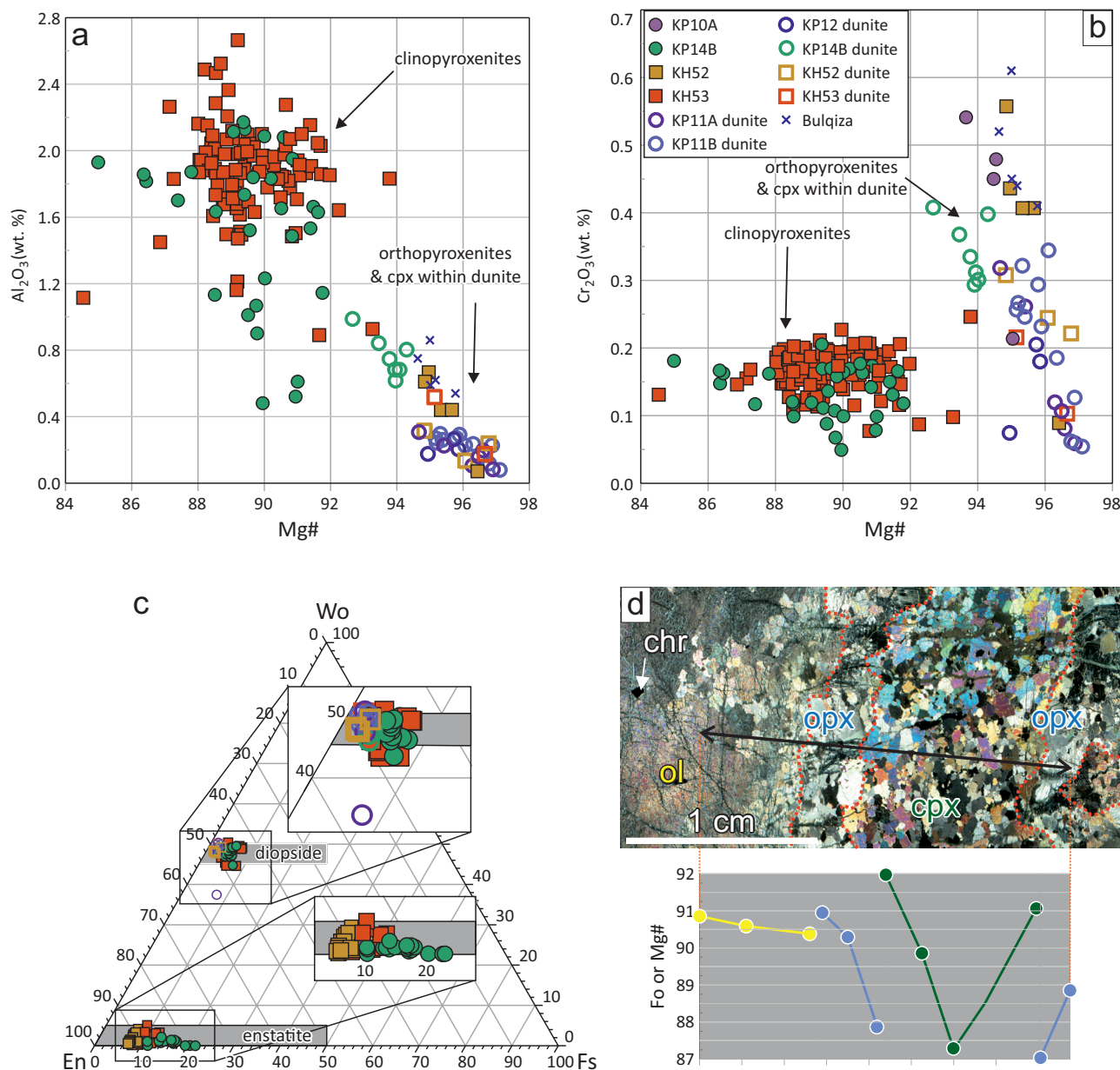


Fig. 7 Chemical features of clinopyroxene (a, b), classification of pyroxenes (c) and chemical profile across clinopyroxenitic vein (d). **a** - Relations between Mg# and Al₂O₃ content. **b** - Relations between Mg# and Cr₂O₃ content. **c** - Pyroxene ternary classification diagram, showing composition of both clino- and orthopyroxene. **d** - Chemical profile across clinopyroxenitic vein, orthopyroxene screen and contacting dunite (KH53) showing variation of Fo in olivine and Mg# in pyroxenes contents. Solid symbols indicate analyses performed within the veins, open symbols represent analyses of interstitial clinopyroxene within dunite. Data for clinopyroxene from Bulqiza dunite is from Xiong et al. (2015).

reaching about 1 km, while in other ophiolitic complexes it is usually much thinner (e.g. in the Oman ophiolite it varies from 0 to 400 m, Ceuleneer 1991; Boudier and Nicolas 1995; Rospabé et al. 2021). Such thick bodies of dunites may be formed due to three processes: 1) decompression melting, 2) cumulate olivine crystallization, or 3) reactive percolation of melt. Decompression melting of peridotite may lead to orthopyroxene removal, but this scenario requires abnormally high mantle potential temperatures exceeding 1600 °C (Walter 2014). Furthermore, intensive melting should increase Fo and NiO contents

in olivine in relation to the protolith (cf. Kubo 2002), while in the Kukes dunites olivine has similar (or lower) Fo content compared to the harzburgites from the same massif, which could have been their protoliths (Fig. 6). Another possibility, fractional crystallization of olivine, would require an unrealistic amount of Mg-rich primitive melt to form over 1 km of dunitic cumulates. Moreover, both mineral and bulk rock composition (i.e. high Fo and low CaO contents in olivine, high MgO and low CaO in bulk rock) and porphyroclastic texture of dunite do not support this hypothesis (Fig. 3, Fig. 6, Fig. 9). The

Tab. 4 Bulk rock chemical composition of Kukes dunites (in wt. % for oxides and LOI and ppm for elements).

Sample Profile position (Fig. 2)	KP10	KP11	KP13
	Vein-contact	0.5m from vein	1.7 m from vein
SiO ₂	37.95	37.59	37.46
TiO ₂	<0.01	<0.01	<0.01
Al ₂ O ₃	0.17	0.10	0.17
Cr ₂ O ₃	0.659	0.723	0.867
Fe ₂ O ₃	9.37	8.92	8.93
MnO	0.13	0.12	0.13
NiO	0.194	0.199	0.200
MgO	43.85	43.93	44.16
CaO	0.19	0.14	0.14
Na ₂ O	<0.01	<0.01	0.01
K ₂ O	<0.01	<0.01	<0.01
P ₂ O ₅	0.01	0.02	<0.01
LOI	7.4	8.2	7.9
Total	99.923	99.942	99.967
Cu	1.3	1.0	1.4
Hf	<0.1	<0.1	<0.1
Ta	<0.1	<0.1	<0.1
Pb	0.2	<0.1	0.1
Th	<0.2	<0.2	<0.2
U	<0.1	<0.1	<0.1
Sc	6	5	5
V	22	18	27
Co	125.9	126.2	126.9
Zn	23	22	21
Rb	<0.1	<0.1	<0.1
Sr	<0.5	<0.5	<0.5
Y	<0.1	<0.1	<0.1
Zr	0.2	0.3	0.5
Nb	<0.1	<0.1	<0.1
Cs	<0.1	<0.1	<0.1
Ba	<1	<1	<1
La	0.4	0.6	0.5
Ce	<0.1	<0.1	0.1
Pr	<0.02	<0.02	<0.02
Nd	<0.3	<0.3	<0.3
Sm	<0.05	<0.05	<0.05
Eu	<0.02	<0.02	<0.02
Cd	<0.1	<0.1	<0.1
Tb	<0.01	<0.01	<0.01
Dy	<0.05	<0.05	<0.05
Ho	<0.02	<0.02	<0.02
Er	<0.03	<0.03	<0.03
Tm	<0.01	<0.01	<0.01
Yb	<0.05	<0.05	<0.05
Lu	<0.01	<0.01	<0.01

last considered process, reaction of peridotite with melt undersaturated in pyroxene, may lead to orthopyroxene removal and crystallisation of secondary olivine. Formation of the Kukes dunite by melt-rock reaction is consistent with low NiO content in olivine (Morgan and Liang 2005; Tursack and Liang 2012). Dunites may be derived

from harzburgites (see below), which form a thick sequence in Kukes (Fig. 1) and have Fo content similar to some of the dunites from the profile (Fig. 6). The NiO content in harzburgitic olivine is in general higher than in the dunitic ones (0.34 to 0.53 and 0.15 to 0.42 wt. % respectively), but some analyses from the distal dunites (KH52 and KH53) also show high NiO content. A continuous range of NiO content from high values (over 0.35 wt. %), typical for harzburgites to low, typical for most of the dunites from the profile (down to 0.15 wt. %), supports reactive genesis of dunites model (Fig. 6). Kelemen (1990) suggested dunite formation due to reaction of the protolithic peridotite with a tholeiitic melt, which in case of the Kukes dunites is contradicted by presence of amphibole inclusions in chromite. We suggest that in Kukes the percolating melt could have had a composition resulting from hybridization between a common silicate melt (e.g. basaltic, boninitic) and a mantle-derived or hydrothermal fluid (cf. Rospabé et al. 2017; Ceuleneer et al. 2022). On the other hand, very high Cr# in chromite may result from re-equilibration with or crystallisation from boninitic melts (Kuroda et al. 1978; Morishita et al. 2011; Saccani and Tassinari 2015). Activity of such melts would cause removal of orthopyroxene from harzburgites and thus reactive dunite formation. Presence of boninitic melts in the mantle seems to be justified by occurrence of boninites in the crustal part of the ophiolite (Dilek et al. 2008). Amphibole inclusions in chromite were related to boninitic melts in Troodos ophiolite on Cyprus, which share also wide range of NiO content within dunite (Merlini et al. 2011).

The chemical composition of olivine forming dunite from the Kukes Massif is extremely variable and significantly wider than that reported for dunites and harzburgites from the SSZ Bulqiza massif (Xiong et al. 2015, Fig. 6). The chemical variability may be explained by the supposed reactive nature of the dunite which formed during multiple reactions of host rock with melts of variable composition (as discussed above). Moreover, the dunites were later cut by magmatic veins which also affected the host rock. Considering this, it seems impossible to establish the exact composition of “primary” (i.e. post-dunite-forming percolation but preceding late veining) dunites and to decipher chemical input of each reaction.

5.2. Chemical relations between veins and host dunite

Veins cutting the Kukes dunites were formed in a context of decreasing temperature, leading to fractional crystallization of the percolating melt and thus the preservation of the footprint of melt migration. Composition of dunitic olivine varies in wide ranges (Fo=87.5–93.3; Fig. 6; Tab. 2); values exceeding 89.5 are interpreted as purely

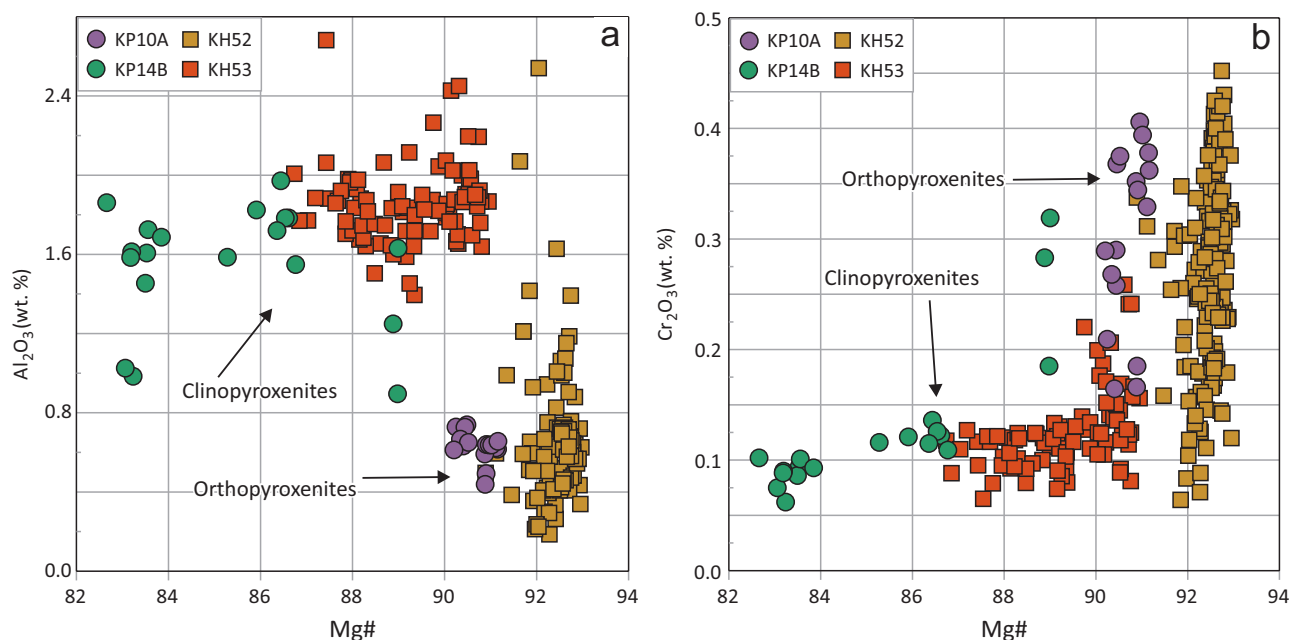


Fig. 8 Chemical composition of orthopyroxene. **a** - Relations between Mg# and Al₂O₃ content. **b** - Relations between Mg# and Cr₂O₃ content. All analyses performed on vein pyroxene.

coming from the mantle in harzburgites and lherzolites and as replacive in most ophiolitic dunites (e.g. Arai 1994). As Fo content decreases during reaction with mafic melt (Morgan and Liang 2005; Tursack and Liang 2012), higher Fo values may indicate olivine less affected by reaction with melt transported by veins. This agrees with field observations in Kukes, where the dunites with

Fo-rich olivine (>90) are distant from the veins; this may also be reflected in lower Fe₂O₃ and higher MgO content in bulk rocks in those dunites (Fig. 9). On the other hand, this criterion is ambiguous, as the chemical composition of the olivine in these “distant” samples partly overlaps with that of olivine from dunites that host veins (Figs 2, 6, and 7d).

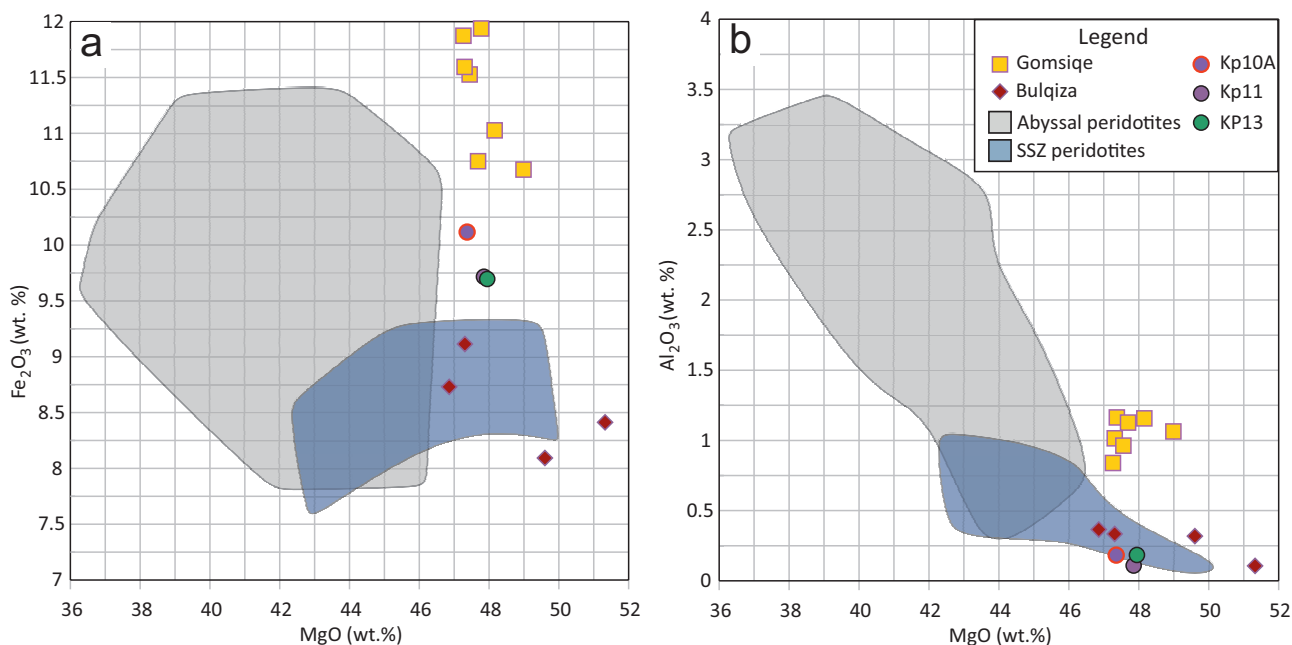


Fig. 9 Bulk rock chemical composition of Kukes dunites. **a** – Relations between MgO and Fe₂O₃ contents. **b** – Relations between MgO and Al₂O₃ contents. Abyssal peridotites field after Niu (2004), data for SSZ peridotites is from Parkinson and Pearce (1998), data for Gomsiqe dunites (western Mirdita) from Wu et al. (2022) and for Bulqiza dunites (eastern Mirdita) from Xiong et al. (2015). All literature data was recalculated to Fe₂O₃ and volatile-free composition.

The composition of chromite grains may give more precise clues on the composition of the “primary” dunite. Cores of some elongated grains (e.g. in dunite KP14B, Fig. 4) have compositions partly overlapping with the harzburgitic spinel ($\text{Cr}\# = 75\text{--}80$, $\text{Mg}\# = 37\text{--}40$) suggesting they are inherited (Fig. 5). However, their rims are more aluminous than high-Cr cores (Al_2O_3 content 15–16 and 10–12 wt. % respectively). In general, chromite grains of this chemical characteristic are supposed to be inherited after harzburgite and constitute a minority. The majority of chromite grains in dunite have isometric form and are more refractory (i.e. less aluminous with the same Cr content) than those in Kukes harzburgites (Fig. 5a). Dunites distant from late veins (>0.3 m) contain spinel with the highest Cr_2O_3 (>56 wt. %) and the lowest Al_2O_3 contents (<8 wt. %), while spinel of more variable composition in terms of Cr, Al (Fig. 5) and Ti contents is proximal to veins. This implies that the highest-Cr, vein-distant chromite may represent “primary”, post-percolation dunite. Isometric forms of chromite suggest magmatic origin. The composition of spinel proximal to veins, together with rims of inherited grains, was modified by later vein-related metasomatism (El Dien et al. 2019). The vein-related modification of chromite was the last significant process recorded by this phase as it contains only minor amounts of magnetite typically formed during serpentinization and lacks chlorite which would point to ferrochromitization (e.g. Grieco and Merlini 2012). Interestingly, in the discussed area chromite is present also in chromitites, however chemical composition of chromitic chromite differs significantly from that of the dunitic one (Fig. 5) which suggest a different origin.

Chemical compositions of minerals forming veins and their cumulative texture confirm magmatic, precipitative origin of the veins. Low TiO_2 (<0.05 wt. % in clinopyroxene) content in KH52 orthopyroxenite suggests a boninitic affinity but further analyses are required to clearly specify character of its parental melt. Similarly, clinopyroxenite may represent a cumulate from high-Ca boninite (cf. Falloon and Danyushevsky 2000; Ceuleneer and le Sueur 2008).

Melts related to the orthopyroxenitic and the clinopyroxenitic veins triggered different metasomatic modifications in the host dunite. Metasomatism related to clinopyroxenitic veins is best seen in dunite (KH53, Fig. 3a), where the rock is cross-cut by a clinopyroxenitic vein enveloped by coarse-grained orthopyroxenes, possibly formed during reaction between silica-saturated melt and olivine (Wang et al. 2016). The chemical compositions of the pyroxenes forming the vein (Figs 7d, 8; Tab. 3) are related to their location within the vein, e.g. Fe content decreases from the centre of the vein towards its contact with dunite. In the dunite, the Cr# of chromite decreases

towards the vein and Ti and Al contents increase (Fig. 5), while in olivine the Fo content decreases sharply with proximity to the vein (Figs 6, 7d; Tab. 2). This chemical characteristic suggests reaction of dunite with silicate mafic melt (e.g. Tursack and Liang 2012).

The olivine in dunite cross-cut by orthopyroxenite (KP10A) has significantly higher Fo content than that from dunite cross-cut by clinopyroxenite (KP14B, Fig. 6). Olivine in dunite cross-cut by orthopyroxenite (KH52, distant from the profile) has the highest Fo content (91.5–92.5). This suggests a limited effect of the orthopyroxenite’s parental melt on Fo content. This could result either from short lifetime of the infiltration process or from the chemical composition of the infiltrating melt. However, the influence of melt within dunites cut by orthopyroxenite is visible in chromite composition: in one of the dunites (KP10A) chromite records progressive Al_2O_3 enrichment (from 11 to 16 wt. %), and in another (KH52) an Al-enriched grain (14 wt. % of Al_2O_3) occurs within the vein.

Metasomatism triggered by infiltration of variable melts in dunites from Kukes had not only cryptic (i.e. changing mineral composition), but also modal expressions and led to formation of wehrlites in vicinity of the described outcrop. Their genesis will be discussed in details elsewhere, but compositions of minerals forming wehrlites partly overlap with those of minerals forming dunites (Figs 5, 6), suggesting their origin due to metasomatism of dunite.

The question remains about the spatial scale at which the metasomatic processes affected country rock. In the case of chromite, differences in chemical composition are most pronounced at the hand specimen scale. Olivine from dunites shows a decrease in Fo content towards the clinopyroxenite veins, while olivine in dunite located further from the clinopyroxenites show no internal differences in Fo content. This suggests that the range of vein interaction with the surrounding rock was just about 0.5 m. This is similar to the observations made in the Oman ophiolite DTZ (e.g. Rospabé 2018; Rospabé et al. 2019). The orthopyroxenite does not appear to have such a large effect on the composition of the dunites at thin-section scale, however bulk rock composition of dunite cut by orthopyroxenite is slightly enriched in Fe compared to distant dunites (Fig. 9). Compared to other massifs within Mirdita ophiolite, the Kukes dunites have higher Fe content than SSZ Bulqiza, but lower than dunites from western, proximal to the rift (Nicolas et al. 2017; Wu et al. 2022) Gomsiqe massif. Those massifs also show a wide variation in chemical composition, which may also be a record of local reactions with infiltrating melts.

The last dunitic phase – the interstitial clinopyroxene – is characterised by very high Mg# (92.5–96.9), negative correlation between Mg# and Al and Cr contents,

positive correlation between Al and Cr contents (Fig. 7). Such composition points to crystallization of clinopyroxene from hydrous fluids (hydrothermal or metasomatic; Python et al. 2007).

6. Conclusions

On the basis of mineral and chemical data on dunites, we propose the following model of dunite evolution and chromite formation in the northern part of the Kukes Massif. Porphyroclastic texture and geochemical features (e.g. high Mg content in silicates) of dunites point to their mantle rather than cumulitic origin. Their protolithic harzburgites reacted with percolating hybrid melt(s) leading to orthopyroxene dissolution and to formation of residual dunite with low-Ni olivine. Reaction of the harzburgite with (possibly) boninites also led to the formation of high-Cr# chromite. After dunite formation activity of another melt was recorded as pyroxenites. Clino- and orthopyroxenitic late veins crystallized, leading to metasomatic increase in Al content in vein-proximal chromite (from around 6–8 up to 18 wt. % Al_2O_3). Orthopyroxenite veins seems to have minor effect on dunitic olivine composition (but is visible in slightly elevated Fe_2O_3 content in bulk rock), whereas interaction with the melt that crystallized as clinopyroxenites caused significant drop in Fo content in olivine (e.g. wide range between 87.5 and 92 in KH53 sample).

Reactions between the dunites and infiltrating melts were probably stopped suddenly and frozen, leaving un-equilibrated rocks proximal to the clinopyroxenitic veins. Orthopyroxenites and olivine in dunite apparently achieved equilibration or the chemical contrast between phases was minor and no reaction occurred. Where the chemical interaction took place, the affected area was limited to ca. 0.5 m around veins. Considering intensive veining and chemical interaction in the discussed relatively small outcrop, we show that local vein-related metasomatism could have transformed a significant part of the massif. The proposed model is the first one discussing the formation of dunite and its later evolution in the northern part of the Kukes Massif. Conclusions presented above may be true for dunitic parts of all the ophiolites worldwide, pointing to need of their careful studies based on numerous samples.

Acknowledgements. We would like to thank Beata Marciniak-Maliszewska, Daniel Buczko and Philippe de Parseval for microprobe analytical assistance and Jacek Puziewicz and Małgorzata Ziobro-Mikrut for constructive discussion. We are grateful to Giovanni Grieco and an anonymous Reviewer whose constructive reviews improved manuscript. This study was financed

from the budget for science in the years 2018–2022 as a research project within “Diamond Grant” program (DI024748).

References

- ABILY B, CEULENEER G (2013) The dunitic mantle–crust transition zone in the Oman ophiolite: Residue of melt–rock interaction, cumulates from high-MgO melts, or both? *Geology* 41: 67–70
- ARAI S (1994) Characterization of spinel peridotites by olivine–spinel compositional relationships: Review and interpretation. *Chem Geol* 113: 191–204
- ARAI S, AKIZAWA N (2014) Precipitation and dissolution of chromite by hydrothermal solutions in the Oman ophiolite: New behavior of Cr and chromite. *Amer Miner* 99: 28–34
- ARAI S, MIURA M (2016) Formation and modification of chromitites in the mantle. *Lithos* 264: 277–295
- BARRA F, GERVILLA F, HERNÁNDEZ E, REICH M, PADRÓN-NAVARTA JA, GONZÁLEZ-JIMÉNEZ JM (2014) Alteration patterns of chromian spinels from La Cabaña peridotite, south–central Chile. *Mineral Petrol* 108: 819–836
- BOUDIER F, NICOLAS A (1995) Nature of the Moho transition zone in the Oman ophiolite. *J Petrol* 36: 777–796
- BUSSOLESI M, GRIECO G, TZAMOS E (2019). Olivine–spinel diffusivity patterns in chromitites and dunites from the Finero Phlogopite-Peridotite (Ivrea–Verbano Zone, Southern Alps): implications for the thermal history of the massif. *Minerals* 9: 75
- BUSSOLESI M, GRIECO G, CAVALLO A, ZACCARINI F (2022) Different tectonic evolution of fast cooling ophiolite mantles recorded by olivine–spinel geothermometry: Case studies from Iballe (Albania) and Nea Roda (Greece). *Minerals* 12(1): 64
- CEULENEER G (1991) Evidence for a paleo-spreading center in the Oman ophiolite: mantle structures in the Maqсад area. In: PETERS TJ, NICOLAS A, COLEMAN RG (eds) *Ophiolite genesis and evolution of oceanic lithosphere. Petrology and Structural Geology*, vol 5. Springer, Dordrecht, pp 147–173
- CEULENEER G, LE SUEUR E (2008) The Trinity ophiolite (California): The strange association of fertile mantle peridotite with ultra-depleted crustal cumulates. *Bull Soc Géol France* 179: 503–518
- CEULENEER G, NICOLAS A (1985) Structures in podiform chromite from the Maqсад district (Sumail ophiolite, Oman). *Miner Depos* 20: 177–185
- CEULENEER G, ROSPABÉ M, CHATELIN T, HENRY H, TILHAC R, KACZMAREK M-A, LE SUEUR E (2022) A Rosetta stone linking melt trajectories in the mantle to the stress field and lithological heterogeneities (Trinity ophiolite, California). *Geology* 50: 1192–1196

- COCOMAZZI G, GRIECO G, TARTAROTTI P, BUSSOLESI M, ZACCARINI F, CRISPINI L, OMAN DRILLING PROJECT SCIENCE TEAM (2020) The Formation of Dunite Channels within Harzburgite in the Wadi Tayin Massif, Oman Ophiolite: Insights from Compositional Variability of Cr-Spinel and Olivine in Holes BA1B and BA3A, Oman Drilling Project. *Minerals* 10(2): 167
- DEER WA, HOWIE RA, ZUSSMAN J (1993) An introduction to the rock-forming minerals. Longman Scientific & Technical, New York, pp 1–696
- DILEK Y, FURNES H (2019) Tethyan ophiolites and Tethyan seaways. *J Geol Soc, London* 176: 899–912
- DILEK Y, SHALLO M, FURNES H (2005) Rift-Drift, Seafloor Spreading, and Subduction Tectonics of Albanian Ophiolites. *Int Geol Rev* 47: 147–176
- DILEK Y, FURNES H, SHALLO M (2008). Geochemistry of the Jurassic Mirdita Ophiolite (Albania) and the MORB to SSZ evolution of a marginal basin oceanic crust. *Lithos* 100: 174–209
- EL DIEN HG, ARAI S, DOUCET LS, LI ZX, KIL Y, FOUGEROUSE D, REDDY SM, SAXEY DW, HAMDY M (2019) Cr-spinel records metasomatism not petrogenesis of mantle rocks. *Nat Commun* 10: 5103
- FALLOON T, DANYUSHEVSKY L (2000) Melting of Refractory Mantle at 1.5, 2 and 2.5 GPa under Anhydrous and H₂O-undersaturated Conditions: Implications for the Petrogenesis of High-Ca Boninites and the Influence of Subduction Components on Mantle Melting. *J Petrol* 41: 257–283
- FURNES H, DILEK Y, ZHAO G, SAFONOVA I, SANTOSH M (2020) Geochemical characterization of ophiolites in the Alpine–Himalayan Orogenic Belt: Magmatically and tectonically diverse evolution of the Mesozoic Neotethyan oceanic crust. *Earth Sci Rev* 208: 103258
- GRIECO G, MERLINI A (2012) Chromite alteration processes within Vourinos ophiolite. *Int J Earth Sci (Geol Rundsch)* 101: 1523–1533
- GONZÁLEZ-JIMÉNEZ J, GRIFFIN W, PROENZA J, GERVILLA F, O'REILLY S, AKBULUT M, PEARSON N, ARAI S (2014) Chromitites in ophiolites: How, where, when, why? Part II. The crystallization of chromitites. *Lithos* 189: 140–158
- HOXHA M, BOULLIER A-M (1995) The peridotites of the Kukes ophiolite (Albania): structure and kinematics. *Tectonophysics* 249: 217–231
- JUNGE M, KOLB AC, WITTENBERG A, SIEVERS H, GEGA D, ONUZI K (2021). Mineralogical characterization of podiform chromitite deposits in the Mirdita Ophiolite, Albania. *Z Dtsch Ges Geowiss* 172 (1): 1–17
- KELEMEN P (1990) Reaction Between Ultramafic Rock and Fractionating Basaltic Magma I. Phase Relations, the Origin of Calc–alkaline Magma Series, and the Formation of Discordant Dunite. *J Petrol* 31: 51–98
- KUBO K (2002) Dunite formation processes in highly depleted peridotite: case study of the Iwanaidake peridotite, Hokkaido, Japan. *J Petrol* 43: 423–448
- KURODA N, SHIRAKI K, URANO H (1978) Boninite as a possible calc–alkalic primary magma. *Bull Volcanol* 41: 563–575
- MERLINI A, GRIECO G, OTTOLINI L, DIELLA V (2011) Probe and SIMS investigation of clinopyroxene inclusions in chromites from the Troodos chromitites (Cyprus): Implications for dunite–chromitite genesis. *Ore Geol Rev* 41: 22–34
- MORGAN Z, LIANG Y (2005) An experimental study of the kinetics of lherzolite reactive dissolution with applications to melt channel formation. *Contrib Mineral Petrol* 150: 369–385
- MORISHITA T, DILEK Y, SHALLO M, TAMURA A, ARAI S (2011) Insight into the uppermost mantle section of a maturing arc: The Eastern Mirdita ophiolite, Albania. *Lithos* 124: 215–226
- NICOLAS A, PRINZHOFFER A (1983) Cumulative or Residual Origin for the Transition Zone in Ophiolites: Structural Evidence. *J Petrol* 24: 188–206
- NICOLAS A, BOUDIER F, MESH I A (1999) Slow spreading accretion and mantle denudation in the Mirdita ophiolite (Albania). *J Geophys Res* 104(B7): 15155–15167
- NICOLAS A, MESH I A, BOUDIER F, JOUSSELIN D, MUCEKU B (2017) Mylonites in ophiolite of Mirdita (Albania): Oceanic detachment shear zone. *Geosphere* 13: 136–154
- NIU Y (2004) Bulk-rock Major and Trace Element Compositions of Abyssal Peridotites: Implications for Mantle Melting, Melt Extraction and Post-melting Processes Beneath Mid-Ocean Ridges. *J Petrol* 45 (12): 2423–2458.
- PARKINSON I, PEARCE A (1998) Peridotites from the Izu–Bonin–Mariana Forearc (ODP Leg 125): Evidence for Mantle Melting and Melt–Mantle Interaction in a Supra-Subduction Zone Setting. *J Petrol* 39 (9): 1577–1618
- PIRARD C, HERMANN J, O'NEILL H (2013) Petrology and Geochemistry of the Crust–Mantle Boundary in a Nascent Arc, Massif du Sud Ophiolite, New Caledonia, SW Pacific. *J Petrol* 54: 1759–1792
- PYTHON M, CEULENEER G, ISHIDA Y, BARRAT J-A, ARAI S (2007) Oman diopsidites: a new lithology diagnostic of very high temperature hydrothermal circulation in mantle peridotite below oceanic spreading centres. *Earth Planet Sci Lett* 255: 289–305
- QUICK JE (1981) The origin and significance of large, tabular dunite bodies in the Trinity peridotite, northern California. *Contrib Mineral Petrol* 78: 413–422
- RODUIT N (2007) JMicroVision: un logiciel d'analyse d'images pétrographiques polyvalent PhD Thesis Université de Genève, pp 1-116
- ROSPABÉ M (2018) Etude pétrologique, géochimique et structurale de la zone de transition dunitique dans l'ophiolite d'Oman: Identification des processus pétrogénétiques à l'interface manteau/croûte. PhD thesis Université Toulouse III, pp 1–628

- ROSPABÉ M, CEULENEER G, BENOIT M, ABILY B, PINET P (2017) Origin of the dunitic mantle–crust transition zone in the Oman ophiolite: the interplay between percolating magmas and high-temperature hydrous fluids. *Geology* 45: 471–474
- ROSPABÉ M, CEULENEER G, GRANIER N, ARAI S, BORISOVA A (2019) Multi-scale development of a stratiform chromite ore body at the base of the dunitic mantle–crust transition zone (Maqsad diapir, Oman ophiolite): The role of repeated melt and fluid influxes. *Lithos* 350–351: 105235
- ROSPABÉ M, CEULENEER G, LE GULUCHE V, BENOIT M, KACZMAREK M-A (2021) The chicken and egg dilemma linking dunites and chromitites in the mantle–crust transition zone beneath oceanic spreading centres: a case study of chromite-hosted silicate inclusions in dunites formed at the top of a mantle diapir (Oman ophiolite). *J Petrol* 62: egab026
- SACCANI E, TASSINARI R (2015) The role of MORB and SSZ magma-types in the formation of Jurassic ultramafic cumulates in the Mirdita ophiolites (Albania) as deduced from chromian spinel and olivine chemistry. *Ofioliti* 40: 37–56
- SACCANI E, DILEK Y, PHOTIADES A (2018) Time-progressive mantle-melt evolution and magma production in a Tethyan marginal sea: A case study of the Albanide–Hellenide ophiolites. *Lithosphere* 10: 35–53
- SHALLO M, DILEK Y (2003) Development of the ideas on the origin of Albanian ophiolites. In: DILEK Y, NEWCOMB S (eds) *Ophiolite Concept and the Evolution of Geological Thought*. *Geol Soc Am, Special Papers* 373: 351–363
- STEBLEZ W (1994) The Chromium Resources of Albania. *Int Geol Rev* 36: 785–795
- SUHR G, HELLEBRAND E, SNOW JE, SECK HA, HOFMANN AW (2003) Significance of large, refractory dunite bodies in the upper mantle of the Bay of Islands ophiolite. *Geochem Geophys* 4: 8605
- TURSACK E, LIANG Y (2012) A comparative study of melt-rock reactions in the mantle: laboratory dissolution experiments and geological field observations. *Contrib Mineral Petrol* 163: 861–876
- WALTER MJ (2014) Melt Extraction and Compositional Variability in Mantle Lithosphere. In: HOLLAND HD, TUREKIAN KK (eds) *Treatise on Geochemistry*. Elsevier, pp 393–419, Second ed
- WANG C, LIANG Y, DYGERT N, XU W (2016) Formation of orthopyroxenite by reaction between peridotite and hydrous basaltic melt: an experimental study. *Contrib Mineral Petrol* 171: 77
- WU W, YANG J, ZHENG J, LIAN D, MILUSHI I, YANG Y, QIU T, RUI H, GUO G, DAI Z, MASOUD AEI (2022) The earliest stage of mantle-melt evolution during subduction initiation: Evidence from the Neo-Tethyan Mirdita Ophiolite, Albania. *Lithos* 434–435: 106937
- XIONG F, JINGSUI YANG J, ROBINSON PT, DILEK F, MILUSHI I, XUA X, CHEN Y, ZHOU W, ZHANG Z, LAI S, TIAN Y, HUANG Z (2015) Petrology and geochemistry of high Cr# podiform chromitites of Bulqiza, Eastern Mirdita Ophiolite (EMO), Albania. *Ore Geol Rev* 70: 188–207